proceedings

Abstract

Thermal Monitoring for Process Control and Parameter Correlation in Laser Powder Bed Fusion of AlSi10Mg †

Ester D'Accardi[1], Davide Palumbo[1], Gianluca Acquistapace[2], Alex Giorgini[2], Francesca Di Carolo[1], Giovanni Santonicola[1] and Umberto Galietti[1].

[1] Department of Mechanics, Mathematics and Management (DMMM), Polytecnic University of Bari, Via Orabona 4, 70125 Bari BA, Italy; ester.daccardi@poliba.it, davide.palumbo@poliba.it, francesca.dicarolo@poliba.it, g.santonicola@phd.poliba.it, umberto.galietti@poliba.it
[2] Valland S.p.a., Via Roccoli 252, 23010 Piantedo SO, Italy; alex.giorgini@valland.it, gianluca.acquistapace@valland.it
* Correspondence: ester.daccardi@poliba.it
† Presented at the 18th International Workshop on Advanced Infrared Technology and Applications (AITA), Kobe, Japan, 15–19 September 2025.

Abstract: Laser Powder Bed Fusion (L-PBF) of AlSi10Mg is challenged by rapid thermal transients and high diffusivity. This study applies a microbolometer-based thermal monitoring system to correlate laser power, scan speed, and build position with thermal features. Results demonstrate reliable detection of defects such as keyhole porosity, supporting real-time process control and quality assurance.

Keywords: monitoring; L-PBF process; AlSi10Mg; statistical analysis; additive manufacturing.

1. Introduction

Laser Powder Bed Fusion (L-PBF) is one of the most advanced additive manufacturing (AM) technologies for producing metal parts with complex geometries and high mechanical performance [1,2]. Among commonly used alloys, AlSi10Mg is particularly valued for its low weight and favorable mechanical properties, making it suitable for aerospace and automotive applications. However, its high thermal diffusivity poses challenges during processing due to rapid temperature changes and complex heat dissipation.

Effective process monitoring is therefore essential to ensure part quality and repeatability. Infrared thermography has emerged as a promising in situ technique for monitoring L-PBF, allowing the capture of thermal signatures related to the melt pool and surrounding powder bed [1,2]. Although the melt pool is typically smaller than the resolution of conventional thermal cameras, previous studies have shown that statistical features extracted from thermal images can successfully correlate process parameters with defect formation [3–6]. This method eliminates the need for direct melt pool visualization or precise knowledge of emissivity and absolute temperature, which are often difficult to determine during processing [3].

Recent research has used thermal data to predict mechanical properties and detect common defects such as keyhole porosity and lack of fusion, employing both statistical analysis and machine learning approaches [1–6].

This work employs a fixed microbolometer thermal system and a Design of Experiments (DOE) varying laser power and speed to analyze thermal features, such as cooling rate, and their correlation with process parameters and defects during L-PBF of AlSi10Mg. The results support real-time monitoring for improved process control and quality assurance.

Citation: To be added by editorial staff during production.

Academic Editor: Firstname Lastname

Published: date

2. Material and Methods

Experiments were conducted on an EOS M290 L-PBF machine equipped with a FLIR A700 camera. The IR system uses a ZnS window and records at 30 fps with a spatial resolution of ~0.6 mm/pixel. Figure 1 illustrates the system and build layout. Small cubes and cylindrical tensile specimens (ASTM E8/E8M) were built with varying power, scan speed, and position on the plate (Table 1). In a dedicated Job, induced keyhole porosity was achieved by reducing scan speed in selected regions, increasing VED from ~74 to ~147 J/mm². For defect areas, a 24° lens was used, improving resolution to ~0.35 mm/pixel.

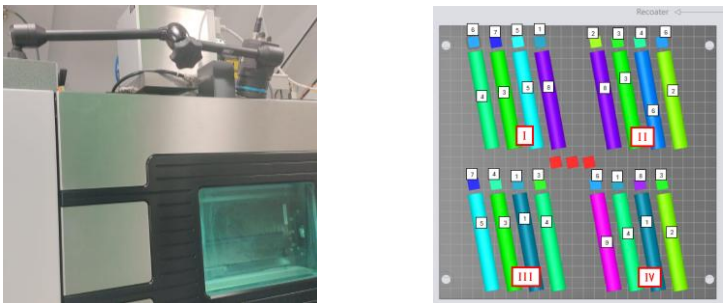

(a) (b)

Figure 1. (a) Adopted set-up for thermal monitoring, and (b) schematic representation of the specimens on the build platform for one Job (Job 1).

Table 1. Design of Experiments (DOE) related to the specific sub-plan, detailing the process parameters and levels analyzed in this study.

Input Parameters	ID	Power (P – W)	Speed (s – mm/s)	Replication	Position
Levels	1	370	1300	layers 1, 2, 3, 4, 5	I
	3	370	700		II
	7	230	1300		III
	9	230	700		IV

The bulk material surrounding the defects was processed using a laser power of 370 W, a scanning speed of 1280 mm/s, and a volumetric energy density (VED) of 74.12 J/mm². In contrast, keyhole porosity was induced in designated defect areas by reducing the scanning speed to 700 mm/s, resulting in an increased VED of 146.83 J/mm². Thermal acquisitions during these tests were performed using a 24° lens, yielding a spatial resolution of approximately 0.35 mm per pixel.

3. Procedure for data analysis

The data analysis procedure involved reconstructing the thermal signal by identifying the maximum signal value associated with the laser scan during material deposition in each region. A 3D sequence was then reconstructed by aligning all frames relative to the maximum (peak) value. Since the laser operates in successive short scan paths and due to the limited track length and high scan speed, secondary peaks may occur as the laser passes nearby shortly after the first exposure.

To avoid interference from overlapping thermal signals, the analysis was restricted to the 10 frames following the identified peak. By considering this window, slope and R^2 [7] were assessed pixel by pixel in both linear and double-logarithmic scales in order to obtain feature maps capable of describing the local cooling behavior in relation to process parameter variations.

From defined rectangular regions of interest (~2000 pixels per sample), a range of statistical features—including mean, standard deviation, minimum, maximum, and selected percentiles—were calculated for each thermal sequence. These features were then

used in ANOVA and regression analyses to identify correlations with process parameters and build position.

4. Results and discussion

Figure 4 presents the results obtained for a specific Job, where at least one specimen with a label ID (as reported in Table 1) is present for each combination of process parameters, considering both the maximum temperature (Figure 2a) and the cooling slope (Figure 4b). In addition, Figure 2c shows the slope map extracted in a double logarithmic scale, which highlights thermal features related to the cooling behavior during process monitoring of specimens with intentionally induced defects — specifically simulating keyhole porosity. As expected, in these defective areas, where scan speed is reduced and volumetric energy density (VED) is increased, the apparent temperatures are higher. This confirms the method's potential for detecting small defects, approximately 1 mm in size.

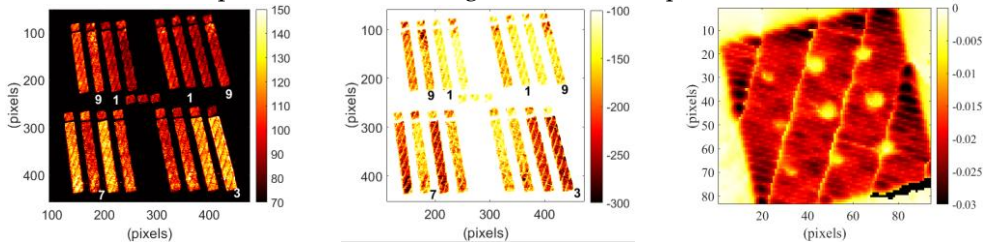

(a) (b) (c)

Figure 2. Extraction of specific thermal features after signal reconstruction (Job 1): (a) maximum apparent temperature and (b) slope in double linear scale and (c) slope map of the specimen exhibiting keyhole porosity in specific selected areas (Job 4).

Qualitatively speaking, significant high apparent temperatures are observed at low scan speeds (ID 3). Additionally, the cooling slope is steeper (more negative) when the scan speed remains at its lowest level. This effect is even more pronounced for the specimen with ID 3, where the laser power is at its highest level. Among the four tested conditions, this one corresponds to the highest VED (Volumetric Energy Density).

The statistical analysis (ANOVA), reported in Table 2, confirmed that power, scan speed, and position had statistically significant effects ($p < 0.001$) on both the maximum temperature and the cooling slope descriptors. In contrast, the replicate factor showed no significant influence ($p > 0.05$), supporting the repeatability and robustness of the measurements collected during the printing of different layers.

Table 2. ANOVA results considering as thermal feature the linear slope and the mean apparent temperature as statistical measure of comparison.

Analysis of Variance (ANOVA)					
Source	**Sum Sq**	**df**	**Mean Sq**	**F**	**Prob>F**
Power	2374	1	2374	16.74	0.0001
Speed	28790.1	1	28790.1	203.03	0
Position	15627.3	3	5209.1	36.74	0
Replication	59	4	14.8	0.1	0.9807
Power : Speed	4283.9	1	4283.9	30.21	0
Error	9843.2	73	141.9		
Total	60918.5	79			

Based on the results obtained from the ANOVA analysis, Figure 3 presents the correlations between thermal features and process parameters with regression models, separating the four positions and evaluating the RMSE, SNR, and R^2 values.

The results show consistently lower variability in Position II, which aligns with the physics of the process. In fact, this quadrant represents the most favourable printing area, with the recoater moving from right to left and the gas flow directed from top to bottom.

In contrast, the other positions exhibit a steeper negative cooling slope across the different parameter combinations, indicating reduced cooling efficiency.

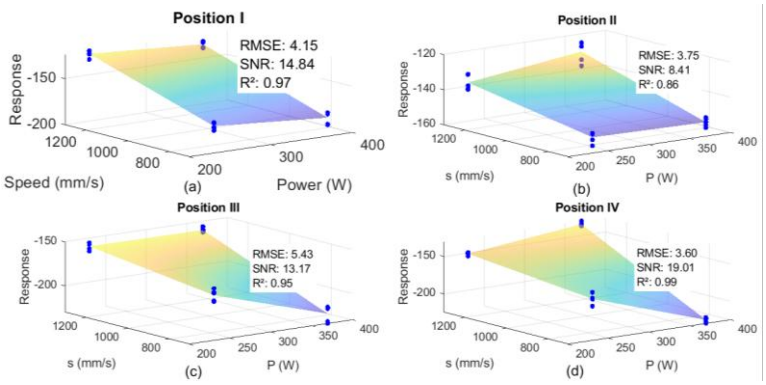

Figure 3. Correlation thermal response vs process parameters considering the different positions in the build platform (a – I position, b – II position, c – III position, d – IV position).

5. Conclusions

The implementation of thermal monitoring via microbolometer sensors enables robust correlation between process parameters and thermal features in L-PBF of AlSi10Mg, despite spatial resolution limitations (~0.6 mm/pixel), without requiring knowledge of the actual emissivity, or monitoring of the melt pool behaviour.

ANOVA results reveal statistically significant effects ($p < 0.001$) of laser power, scan speed, and build position on thermal features such as maximum apparent temperature and cooling slope, with linear models capable of describing this correlation. Moreover, localized detection of keyhole porosity defects, approximately 1 mm in size, is demonstrated through slope map analysis, confirming the system's capability for in-situ defect identification and process control. Future work will focus on developing advanced real-time algorithms for automated defect prediction, adaptive process parameter adjustment and mechanical properties estimation.

Author Contributions: Conceptualization, E.D. and U.G.; methodology, E.D., G.S., F.C., D.P. and U.G.; formal analysis, E.D.; investigation, E.D., G.S. and F.C.; data curation, E.D.; writing—original draft preparation, E.D.; writing—review and editing, G.A., G.S., F.C., D.P. and U.G.; supervision, U.G., D.P. and A.G.; project administration, U.G. and A.G.; funding acquisition, U.G.

Funding: This research was funded by the project TO ZERO - Towards Zero Waste In Aluminium Body-In-White Manufacturing a valere sulle agevolazioni previste dal Decreto Ministeriale 31 dicembre 2021 (Primo sportello) del MIMIT – Accordi per l'innovazione, CUP: B99J23002030005.

Conflicts of Interest: "The authors declare no conflicts of interest."

References

1. Oster, S., Breese, P. P., Ulbricht, A., Mohr, G., & Altenburg, S. J. (2024). A deep learning framework for defect prediction based on thermographic in-situ monitoring in laser powder bed fusion. *Journal of Intelligent Manufacturing*, *35*(4), 1687-1706.
2. Errico, V., Palano, F., & Campanelli, S. L. (2024). Advancing powder bed fusion-laser beam technology: in-situ layerwise thermal monitoring solutions for thin-wall fabrication. Progress in Additive Manufacturing, 1-15.
3. D'Accardi, E., Chiappini, F., Giannasi, A., Guerrini, M., Maggiani, G., Palumbo, D., & Galietti, U. (2024). Online monitoring of direct laser metal deposition process by means of infrared thermography. *Progress in Additive Manufacturing*, *9*(4), 983-1001.
4. Scheuschner, N., Heinrichsdorff, F., Oster, S., Uhlmann, E., Polte, J., Gordei, A., & Hilgenberg, K. (2023). In-situ monitoring of the laser powder bed fusion process by thermography, optical tomography and melt pool monitoring for defect detection. In *Lasers in Manufacturing Conference 2023* (pp. 1-10).
5. Chand, K., Fritsch, T., Oster, S., Ulbricht, A., & Bruno, G. (2025). Review on image registration methods for the quality control in additive manufacturing. *Progress in Additive Manufacturing*, 1-27.
6. Mazzarisi, M., Angelastro, A., Latte, M., Colucci, T., Palano, F., & Campanelli, S. L. (2023). Thermal monitoring of laser metal deposition strategies using infrared thermography. *Journal of Manufacturing Processes*, *85*, 594-611.
7. Dell'Avvocato, G., Gohlke, D., Palumbo, D., Krankenhagen, R., & Galietti, U. (2022, May). Quantitative evaluation of the welded area in Resistance Projection Welded (RPW) thin joints by pulsed laser thermography. In *Thermosense: Thermal Infrared Applications XLIV* (Vol. 12109, pp. 152-165). SPIE.